Relative contribution of different potentials in the estimation of directed flow

A dissertation submitted in partial fulfillment of the requirement for the award of the degree of

Masters of Science

In

PHYSICS

Under the esteemed guidance of

Dr. Suneel Kumar

Submitted by

Ankita Sharma
Roll no.-301004020

School of Physics and Materials Science
Thapar University
Patiala- 147004 (PUNJAB)
(INDIA)

Dedicated

To

My parents

CERTIFICATE

This is to certify that Ms. Ankita Sharma, Roll No. 301004020 has worked on this dissertation report as a partial fulfillment for award of the degree of **MASTERS OF SCIENCE** in physics. I certify that the matter embodied in this report is of candidate's own record and not submitted to any other university in any part or full form for the award of such a degree.

S Kumar

(Dr. Suneel Kumar)
Associate Professor
SPMS, Thapar University,
Patiala.

Countersigned by:

Dr. Kulvir Singh
(Head)
School of physics and Material Science,
Thapar University,
Patiala.

Dr. S. K. Mohapatra
Dean of academic Affairs
Thapar University,
Patiala.

ACKNOWLEDGEMENT

I owe my deepest gratitude to **Dr. Suneel Kumar**, *my worthy supervisor*, who has been an inspiration during my research work. Without him, this dissertation would not have been possible. I thank him for his patience and encouragement that carried me on through difficult times, and for his insights and suggestions that helped to shape my research skills. I express my sincere thanks to him for his valuable guidance in carrying out work under his effective supervision, encouragement and cooperation. His visionary thoughts have influenced me greatly. His dynamical attitude has empowered me with zeal of energy to conquer the minor details of my research work.

I also thank Dr Kulvir Singh, Head, School of Physics and Material Science for his support and providing facilities.

A special word of thanks to Ms Mandeep Kaur, Ms Anupriya Jain and Mr. Karan Singh Vinayak Research Scholars for the help and valuable suggestions whenever I needed out of their busy schedule.

Special thanks are due to all my friends and the staffs at the School of Physics and Materials Sciences for providing me a friendly atmosphere and encouraging me throughout this work.

I am deeply thankful to my family, their moral support and patience has bared fruit through completion of this dissertation.

Ankita Sharma

Ankita Sharma
Roll no. 301004020
Date: 9.7.12

ABSTRACT

The present work deals with the theoretical study of directed flow in heavy ion collisions at intermediate energies. We present a complete systematic study of directed flow for asymmetric colliding nuclei for heavy ion reactions in the energy range between 60 (MeV/nucleon) and 140 (MeV/nucleon) by using hard equation of state. This study is performed within an isospin-dependent quantum molecular dynamics (IQMD) model. We envision an interesting outcome for asymmetric colliding nuclei. Also the effect of different potentials on heavy ion collisions has been studied.

TABLE OF CONTENTS

CHAPTER 1

INTRODUCTION

1.1 Heavy-ion Physics

Heavy ion physics is the branch of physics which deals with the phenomenon that occur when two heavy nuclei are brought into close contact such that the nuclear forces that hold neutrons and protons together within the nucleus are felt by other nucleons. For low density phenomena, we study low energy nuclear physics (≤ 10A MeV). The low energy heavy-ion reactions give unique possibility to look for the nuclear interactions, fusion-fission, cluster radioactivity, formation of super heavy nuclei, and possibilities of synthesis of super heavy elements, halo nuclei [1,2] etc. Thus low energy nuclear physics focuses mainly on the structure of nuclei. At low energies, the available free phase space is very small, therefore 98% of attempted collisions are blocked and the whole dynamics at low energies is due to mean field. At high energies (> 2 GeV/nucleon) there is a presence of large free phase space, so only 4% of attempted collisions are blocked and the dynamics is due to the collisions. At intermediate energies (10 MeV/nucleon ≤ E ≤ 2 GeV/nucleon) both collisions and mean field are taken into considerations. The main aim of studying heavy - ion collisions at intermediate energies is to extract some information on equation of state. Reactions at intermediate energies are violent enough to excite the system to very high temperature leading to the break -up of initial correlations among nucleons, but not strong enough to break the internal structure of nucleons or hadrons.

The normal nuclear matter is described by the physics at normal nuclear density and low temperature. Figure 1, shows that the phase transition between the nuclear liquid and a gas of nucleons is not the only phase transition that we study in heavy-ion collisions. At even higher temperature and densities, nucleons themselves can undergo a phase transition. Nuclear matter can appear in different phases (i.e. liquid Hadron Gas and Quark-Gluon Plasma phases) depending upon temperature and density. The normal nuclear matter at ($\rho = \rho_o$, T = 0) represents the liquid phase. The liquid gas

phase (LGP) transition region is characterized by the temperature below ≈ 15 MeV and densities ($\frac{\rho}{\rho_o} < 1$).

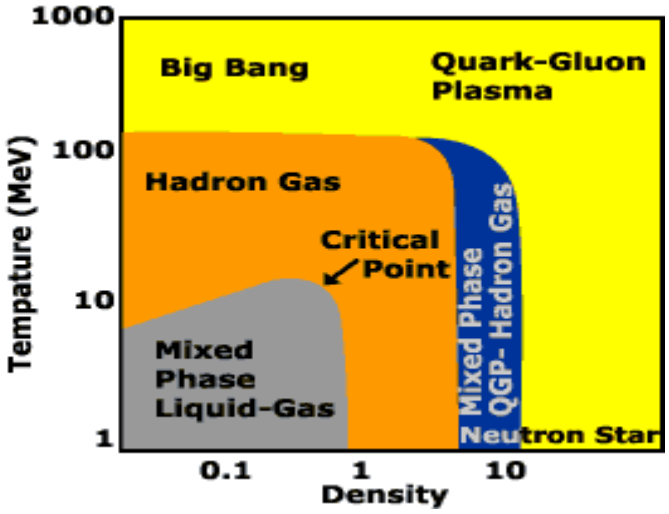

FIG.1. The phase diagram for nuclear matter. The horizontal axis shows the matter density, and the vertical axis shows the temperature.

A highly dense and hot region corresponds to Quark-Gluon Plasma (QGP) phase. The hadron gas (HG) phase exists at intermediate temperature and density. Major research efforts at BNL (Brookhaven National Laboratory) in New York and at CERN (Conseil Europeen pour la Recherche Nucleaire) in Switzerland are directed toward establishing the conditions for creating this phase transition and observing its signatures.

Heavy ion collisions at intermediate energies offers excellent opportunities to study nucleon - nucleon collisions, phenomena's such as multi-fragmentation, collective flow and nuclear stopping etc. All these phenomena are studied in the literature time independently. As my topic is concerned with multi-fragmentation and flow so we will discuss these two processes in detail.

1.2 Phenomena's at intermediate energies

Multi-fragmentation: When two nuclei collide, the dense and strongly interacting nuclear matter gets condensed by emitting large number of fragments which include free nucleons (FN's), light charged particles (LCP's) and intermediate mass fragments

(IMF's). This phenomenon of breakup of nuclear matter is termed as multi-fragmentation. It depends on the number of entrance channel parameters such as incident energy (E), collision geometry (b), mass of colliding nuclei (M_P, M_T), mass asymmetry ($\eta = (A_T - A_P)/(A_T + A_P)$).

Collective Flow: The collective flow is characterized by the space and momentum correlations of dynamic origin. Basically, the directed and elliptical flows are the two observables to study the collective flow. The directed transverse flow, is very sensitive to the physical scenario. At low incident energy, directed transverse flow is attractive, but turns repulsive at higher incident energies. The directed flow seems to be constrained only along the reaction plane which is due to the bounce-off of the compressed matter. However, the elliptical flow is more suited to study the collective flow which is squeeze-out of the spectator matter out of the reaction plane [3].

1.3 Experimental &Theoretical Review

Many theoretical and experimental efforts have been made in studying the process of multi - fragmentation, collective flow etc. in Heavy - ion collisions. Experimentally, the FOPI and ALADIN groups at GSI studied the multi-fragmentation process over a wide range of masses from 12 to 208 units for wide range of incident energies from 100 to 1000 MeV/nucleon.

INDRA group at GANIL (France) is also one of the leading group in this field. The main interest of INDRA collaboration at GANIL is to study the collisions where large multiplicities of the nucleons are observed in the exit channel and they have studied the influence of different parameters on multifragmentation including role of size of system in entrance channel, Coulomb instabilities etc. On the other hand the entrance channel effects are studied by keeping the total mass equal to 250 units. A detailed theoretical study of INDRA experimental findings was carried out by Aichelin and coworkers [4].

Theoretically, Plastic Ball group at the Bevalac in Berkley, National Superconducting Cyclotron Laboratory (NSCL) at MSU focuses on the study of flow. At present, several experimental groups are engaged in extracting information of nuclear EOS

from multifragmentation and nuclear flow/fragment flow. Many body nuclear dynamics group at INDIANA University Bloomington, USA studied the role of nuclear equation of state (EOS) in particular how the density dependence of the symmetry energy affects the properties of nuclear matter [5].

Now we will study about different potentials.

1.4 Different kinds of potentials

- **Yukawa Potential:** It is a potential of the form

$$V_{Yukawa}(\mathbf{r}) = -g^2\left(\frac{e^{-\mathrm{mr}}}{r}\right) \qquad 1.1$$

g represents the magnitude of scaling constant, r is the radial distance to the particle. This potential is monotonously increasing, implying that the force is always attractive. In interaction between a meson field and a fermion field, g is equal to coupling constant between those fields. Hideki Yukawa showed in 1930s that such a potential arises from the exchange of a massive scalar field such as field of the pion whose mass is m. Since the field mediator is massive, the corresponding force has a certain range, which is inversely proportional to the mass.

Relation to Coulomb potential

If the mass is zero, then the Yukawa potential becomes equivalent to a Coulomb potential, and the range is said to be infinite. As the mass approaches 0, the exponential term goes to 1,

$$\mathbf{m} \to \mathbf{0} : e^{-mr} \to e^{0} \to \mathbf{1}$$

So in this limit the equation,

$$V_{Yukawa}(\mathbf{r}) = -g^2\left(\frac{e^{-\mathrm{mr}}}{r}\right)$$

becomes a form of the Coulomb potential,

$$V_{Coulomb}(\mathbf{r}) = -g^2\,\frac{1}{r} \qquad 1.2$$

A comparison of the long range potential strength for Yukawa and Coulomb is shown in Figure 1. It can be seen that the Coulomb potential has effect over a greater distance whereas the Yukawa potential goes to zero rather quickly.

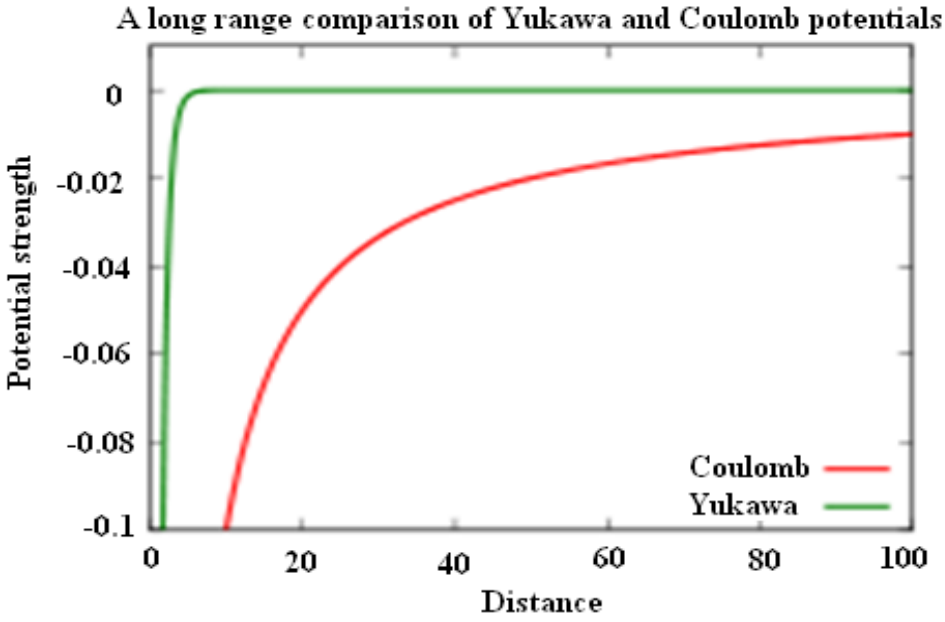

Figure 1: A "long-range" comparison of Yukawa and Coulomb potentials' strengths where g=1.

- **Coulomb Potential:** It is an effective pair potential that describes interaction between two point charges. It acts along the line connecting two charges.

$$V_{Coulomb} = \frac{1}{4\pi\varepsilon_o}\frac{q_1 q_2}{r} \qquad 1.3$$

r is the distance between two ions, ε_o is electrical permittivity, q_1, q_2 are the electric charges. Two oppositely charged particles will give an attractive potential whereas if both particles are of same sign then potential is repulsive.

The Coulomb force between the two molecules is

$$F_{Coulomb} = -\frac{1}{4\pi\varepsilon_o}\frac{q_1 q_2}{r} \qquad 1.4$$

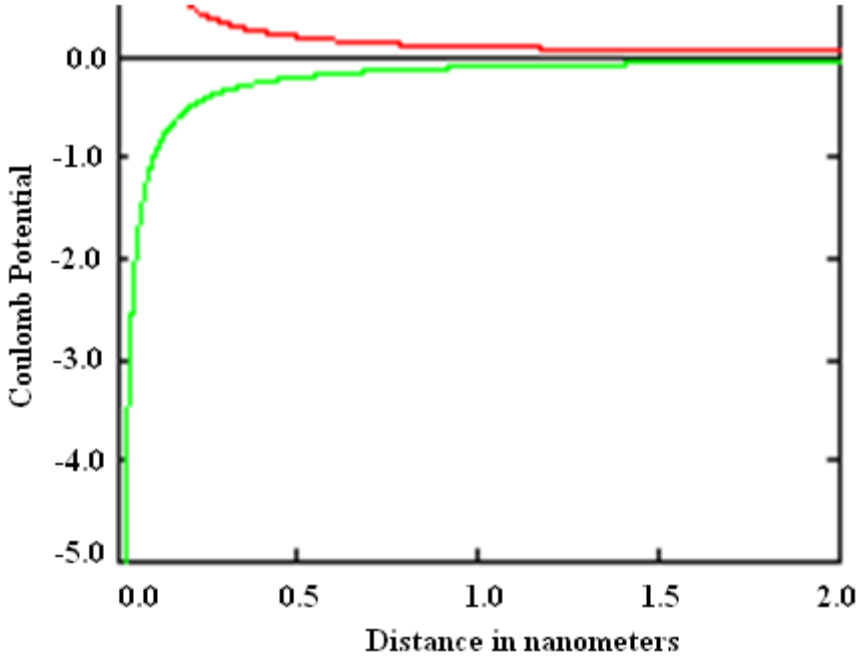

Figure 2: The Coulomb potential. The bottom curve represents the interaction between two particles of opposite charges and the top curve represents the interaction of particles of equal charges.

➢ **Momentum dependent interactions:** These interactions act during the initial phase of the reaction when relative momentum is quite large. The particles propagating with momentum dependent interactions are accelerated in the transverse direction during the early phase of the reaction. As a result fewer collisions take place and the transverse flow increases considerably. The momentum dependence of equation of state has also attracted a lot of considerations, momentum dependent interactions are found to affect the collective flow quite drastically.

➢ **Symmetry Potential:** Symmetry is that energy at which protons in the nucleus tends to be neutrons and vice-versa. The symmetry energy (E_{sym}) of nuclear matter characterizes how energy rises as one moves away from equal number of neutrons and protons. Nuclear symmetry energy which encodes energy related to

neutron-proton asymmetry in equation of state of nuclear matter, is a fundamental quantity currently under intense investigation in both nuclear physics and astrophysics. Despite much effort made both experimentally and theoretically, our current knowledge about E_{sym} (ρ) is still poor. There are two different type of the density dependence of the symmetry energy. One, where the symmetry energy increases monotonically with increasing density ("stiff" dependence) and the other, where the symmetry energy increases initially upto normal nuclear density and then decreases at higher densities ("soft" dependence).

The equation for density dependence of symmetry energy can be written as

$$C_{sym}(\rho) = C^{o}_{sym}\left(\frac{\rho}{\rho_o}\right)^{\gamma} \text{ (MeV)} \qquad 1.5$$

where C^{o}_{sym}, represents the value of the symmetry energy at normal density , γ represents the stiffness of the symmetry energy.

The study of collective transverse flow in nucleus-nucleus collisions can provide information about the nuclear equation of state (EOS). Transport models have been used to describe collective transverse flow, these models predict that collective transverse flow in the reaction plane disappears at an incident energy, termed as balance energy E_{bal}, where the attractive scattering (dominant at energies around 10 MeV/nucleon) balances the repulsive interactions (dominant at energies around 400 MeV/nucleon). The disappearance of directed transverse flow has been well established through many experiments. Comparison of the measured impact parameter dependence of the balance energy with predictions from isospin dependent quantum molecular dynamics model calculations demonstrated better agreement.

Our aim in this dissertation is to see the contribution of different potentials on directed flow. Also we have compared our theoretical results with experimental data.

Chapter 2

Methodology

2.1 Isospin-dependent Quantum Molecular Dynamics (IQMD) Model

Quantum Molecular Dynamics model contains two dynamical ingredients; the density dependent mean field and the in-medium nucleon-nucleon cross-section. In order to describe the isospin dependence appropriately, the QMD model should be modified properly. Considering the isospin effects in mean field, two-body collision and Pauli blocking, important modifications in QMD have been made to obtain an isospin-dependent quantum molecular dynamics (IQMD) [6]. The isospin-dependent quantum molecular dynamics model treats different charge states of nucleons, deltas and pions explicitly, as inherited from the Vlasov-Uehling-Uhlenbeck (VUU) model [7]. This model has been used successfully for the analysis of large number of observables from low to relativistic energies. The isospin degree of freedom enters into the calculations via cross-sections and mean field [7]. The cross-section for neutron-neutron collisions are assumed to be equal to proton-proton cross-sections.

This model includes three important steps:

- In the first step, nuclei is generated. This is known as initialization.
- In second step, nuclei propagate under the influence of surrounding mean field. This is known as propagation.
- Finally, nucleons are bound to collide if they come too close to each other. This is dubbed as collisions.

2.1.1 Initialization

In this model, baryons are represented by Gaussian-shaped density distributions

$$f_i(\mathrm{r, p, t}) = \frac{1}{\pi^2 \hbar^2}\, e^{-(r-r_i(t))^2/2L} e^{-(p-p_i(t))^2 .2L/\hbar^2} \qquad 2.1$$

Here Gaussian width L is regarded as a description of the interaction range of particle. The system dependence of L has been introduced in IQMD in order to obtain

maximum stability of the nucleonic density profiles. For the heavier system (e.g. $^{197}_{79}$Au + $^{197}_{79}$Au), its value is 8.66 fm^2 and for lighter system (e.g. $^{40}_{20}$Ca + $^{40}_{20}$Ca), its value is 4.33 fm^2. Nucleons are initialized in a sphere with radius R =1.12$A^{1/3}$ fm, according to liquid drop model. Each nucleon has a volume of h^3, so that phase space is uniformly filled. The Fermi momentum p_F depends on the ground state density. For ρ_o = 0.17 fm^{-3}, it has a value of about 268 MeV/c. Pion production is treated via the delta resonance. This model performs a Lorentz contraction of the nucleus coordinate distribution, which becomes important at higher energies.

2.1.2 Propagation

The successfully initialized nuclei are then boosted towards each other with proper center of mass velocity using relativistic kinematics. The nucleons of target and projectile interact via two and three-body Skyrme forces, a Yukawa potential and momentum dependent interactions. The isospin degree of freedom is treated explicitly by employing a symmetry potential and explicit Coulomb forces between protons of colliding target and projectile. This helps in achieving correct distribution of protons and neutrons within nucleus.

The hadrons propagate under the influence of the potential in Hamiltonian's equation of motion:

$$\frac{dr_i}{dt} = \frac{d\langle H\rangle}{dp_i} \quad ; \quad \frac{dp_i}{dt} = -\frac{d\langle H\rangle}{dr_i} \qquad 2.2$$

Potentials used in IQMD

A total Hamiltonian function with a kinetic energy T and a potential energy V is given by

$$\langle H\rangle = \langle T\rangle + \langle V\rangle$$

$$= \Sigma \frac{p_i^2}{2m_i} + \sum_i \sum_{j>i} \int f_i(\mathrm{r}, \mathrm{p}, \mathrm{t})\, V^{ij}(r', \mathrm{r}) \times f_j(r', p', \mathrm{t})\mathrm{d}r\mathrm{d}r'\mathrm{d}p\mathrm{d}p' \quad 2.3$$

The baryon-baryon potential V^{ij}, in above relation, reads as:

$$V^{ij}(r' - \mathrm{r}) = V^{ij}_{Skyrme} + V^{ij}_{Yukawa} + V^{ij}_{Coulomb} + V^{ij}_{MDI} + V^{ij}_{Sym}$$

$$= (t_1\delta(r' - \mathrm{r}) + t_2\delta(r' - \mathrm{r})\rho^{\gamma-1}(\frac{r'+r}{2}))$$

$$+ t_3 \frac{\exp(\frac{|r'-r|}{\mu})}{(\frac{|r'-r|}{\mu})} + \frac{Z_i Z_j e^2}{|r'-r|} + t_4 ln^2[t_5(p_i' - p)^2 + 1]\delta(r' - r)$$

$$+ t_6 \frac{1}{e_o} T_3^i T_3^j \delta(r_i' - r_j) \quad 2.4$$

Here Z_i and Z_j corresponds to the charges of i^{th} and j^{th} baryon, and T_3^i , T_3^j are their respective components. The finite range Yukawa potential with t_3 = -6.7 MeV is important to stabilize the surface of a finite nucleus. The parameters **μ** and t_1, ……., t_6 are adjusted to the real part of the nucleonic optical potential. Other baryonic potentials like V^{ij}_{Skyrme} and V_{MDI} are isospin- independent. For nucleon optical potential depending upon the density, standard Skyrme-type parameterization is employed as:

$$V_{local} = \frac{\alpha}{2}(\frac{\rho}{\rho_o}) + \frac{\beta}{\gamma+1}(\frac{\rho}{\rho_o})^2 \quad 2.5$$

The mean field notation with the parameters α, β, γ has been chosen for reasons of simplicity and in order to compare the parameters with those used in VUU-BUU calculations.

Two different nuclear equation of state (NEOS) have been implemented i.e. A hard NEOS with a compressibility of 380 MeV and a soft NEOS with a compressibility of 200 MeV. The Yukawa potential in IQMD is very short ranged and weak. Yukawa

forces also stabilize the nuclei due to the increase of the interaction range as compared to a δ-like Skyrme potentials. This results in the reduction of fluctuations.

2.1.3 Nucleon-Nucleon (NN) Collisions

The binary nucleon-nucleon collisions are included by employing the collision term of well known VUU-BUU equation [7]. The binary collisions are done stochastically, in a similar way as in the Cascade models. During the propagation, two nucleons collide if their minimum distance d fulfills

$$d = |r_i - r_j| \leq \sqrt{\frac{\sigma_{tot}}{\pi}},\ \sigma_{tot} = \sigma(\sqrt{s}, \text{type}), \quad 2.6$$

" type" denotes the ingoing collision partners (N-N, N-Δ, N-π,..).

2.1.3.1 Pauli blocking

Whenever a collision occurred, in the phase space we assume that each nucleon occupies a six dimensional sphere with a volume of $h^3/2$ and then calculate the phase volume V, of the scattered nucleons being occupied by the rest nucleons with the same isospin as that of the scattered ones. Then we compare $2V/h^3$ with a random number and decide whether the collision is blocked or not. So the Pauli blocking is isospin dependent. Pauli blocking of neutron and proton is treated separately.

In addition, Pauli blocking (of the final state) of baryons is taken into account by checking the phase space densities in the final states. The final phase space fractions P_1 and P_2 which are already occupied by other nucleons are determined for each of the scattering baryons. The particular attempt for a collision is then blocked with the probability

$$P_{block} = 1 - (1 - P_1)(1 - P_2) \quad 2.7$$

Whenever an attempted collision is blocked the scattering partners maintain the original momenta prior to scattering. Delta decays are checked in an analogous fashion with respect to the phase space of the resulting nucleon. Furthermore,

parametrized free pn and pp cross- sections are used instead of an averaged nucleon-nucleon cross-sections. The total cross-section is the sum of the elastic and all inelastic cross-sections.

$$\sigma_{tot} = \sigma_{el} + \sigma_{inel}$$

$$= \sigma_{el} + \Sigma_{channels}\sigma_i \qquad 2.8$$

The following inelastic reactions might influence the dynamics of the collision and are explicitly taken into account:

(a) N + N → Δ + N (hard- delta production)

(b) Δ → N + π (delta decay)

(c) Δ + N → N + N (delta absorption)

(d) N + π → Δ (soft- delta production)

Experimental cross-sections are used for processes (a) and (d), as well as for the elastic NN collisions. Inaccessible reactions like $\Delta N \rightarrow NN$ are calculated from their reverse reactions (like NN → ΔN) using modified detailed balance formula [8]. The conventional detailed balance formula is only correct for particles with infinite lifetimes (zero width). The elastic nucleon-nucleon scattering angular distribution is taken to be

$$\frac{d\sigma_{el}}{d\Omega} \approx \exp[A(s)t] , \qquad 2.9$$

Where t is $-q^2$, the transverse momentum transfer and

$$A(s) = 6\frac{[3.65(\sqrt{s}-1.8766)]^6}{1+[3.65(\sqrt{s}-1.8766)]^6} \qquad 2.10$$

$\sqrt{s}$ is the c.m energy in GeV and A is given in $(\frac{GeV}{c})^{-2}$.

The isospin degree of freedom play an important role especially for the particle production. The parameterization suggested by Huber and Aichelin [9] is used: fitted differential cross-sections are extracted from one boson- exchange (OBE) calculations:

$$\frac{d\sigma_{in}}{d\Omega} \approx \text{a(s)exp[b(s)cos}\theta] \qquad 2.11$$

The a(s) and b(s) are functions of $\sqrt{s}$ and vary in their definition for different intervals of $\sqrt{s}$. θ is the polar angle.

x = $\sqrt{s}$ (GeV)	a (fm)	B
2.104 – 2.12	$294.6(x-2.014)^{2.578}$	$19.71(x-2.014)^{1.551}$
2.12 – 2.43	$\frac{0.01224}{(x-2.225)^2+0.004112}$	$19.71(x-2.014)^{1.551}$
2.43 – 4.50	$(2.343/x)^{43.17}$	$33.41\arctan(0.5404(x-2.146)^{0.9784})$

These isospin effects in the IQMD are found to vary the results, one obtained with QMD model.

2.2 Method of Clusterization

Minimum Spanning Tree (MST) method

In MST, two nucleons share the same fragment if their centroids are closer than a distance d_{min} ,

$$|r_i - r_j| \leq d_{min} \qquad 2.12$$

Where r_i and r_j are the spatial positions of both nucleons. The minimum distance has been used as a free-parameter which varies between 2-4 fm. It has small effect on multi-fragmentation [10,11]. This method will give a single big fragment during the early stage of the reaction where density is quite high and the interactions among the nucleons are still active.

Chapter 3

DIRECTED FLOW

3.1 Introduction

Anisotropic flow (the directed flow and elliptic flow) is of interest in theoretical and experimental investigations on nuclear reaction dynamics in intermediate and high energy heavy-ion collisions. Anisotropic flow is defined as the different n^{th} harmonic coefficient v_n of an azimuthal Fourier expansion of the particle invariant distribution [12]

$$\frac{dN}{d\phi} \propto 1+ 2\sum_{n=1}^{\infty} v_n \cos(n\phi). \quad 3.1$$

where ϕ is the azimuthal angle between the transverse momentum of the particle and the reaction plane. The Ist harmonic coefficient v_1 represents the directed flow,

$v_1 = < cos\phi > = < \frac{P_x}{P_t} >$, where $P_t = \sqrt{P_x^2 + P_y^2}$ is transverse momentum. v_2 represents elliptic flow which characterizes the eccentricity of the particle distribution in momentum space

$$v_2 = < \cos(2\phi) > = < \frac{P_x^2 - P_y^2}{P_t^2} > \quad 3.2$$

and v_y represents the 4^{th} momentum anisotropy,

$$v_4 = < \frac{P_x^4 - 6P_x^2P_y^2 + P_y^4}{P_t^4} > \quad 3.3$$

3.2 Results and Discussion

For the present study we simulate several thousands events for the systems $^{58}_{28}$Ni + $^{58}_{28}$Ni, $^{58}_{26}$Fe + $^{58}_{26}$Fe at incident energies ranging from 60 to 140 MeV/nucleon in steps of 20 MeV/nucleon. The impact parameter ($\hat{b} = b/b_{max}$) is ranging from 0.28 to 0.56. We use a hard equation of state (EOS). We are using a reduced cross-section $\sigma_{red} = 0.9\,\sigma_{NN}$. The time evolution of the reaction is followed upto the saturation time of heavy-ion reaction (i.e 200 fm/c). We can get the information about E_{bal} from P_X/A plots, where we plot $< P_X/A >$ as a function of rapidity distribution, where rapidity distribution is written as

$$Y(i)=\frac{1}{2}\ln\frac{E(i)+P_z(i)}{E(i)-P_z(i)} \quad 3.4$$

Where E(i) and $P_Z(i)$ are total energy and longitudinal momentum of i^{th} particle. We have also used directed transverse flow $< P_x^{dir} >$ to get information about E_{bal}. Directed flow is defined as

$$< \mathrm{P_x^{dir}} > = \frac{1}{A}\sum_i^A sign\{Y(i)\}\, P_x(\mathrm{i}) \quad 3.5$$

$P_x(i)$ is transverse momentum of i^{th} particle along x – direction and Y(i) is rapidity distribution. $< \mathrm{P_x^{dir}} >$ is defined over entire rapidity range.

Figure.3.1 shows the effect of different kinds of potential on the scaled density of the colliding nuclei. Acronym sy stands for Skyrme + Yukawa, syc stands for Skyrme + Yukawa + Coulomb, sycm stands for Skyrme + Yukawa + Coulomb + Momentum dependent interactions, sycms stands for Skyrme + Yukawa + Coulomb + Momentum dependent interactions + Symmetry potential. Here the impact parameter is taken to be 0.28 and the energy is 100 MeV/nucleon. It is seen that the results for sy and syc in both the systems are found to be equal but on adding momentum dependent interactions to syc, the density starts decreasing.

Fig.3.2. shows the collision rate $\frac{\mathrm{dN_{coll}}}{\mathrm{dt}}$ for impact parameter $b/b_{max} = 0.28$ at 100 MeV/nucleon. We find that coulomb interactions decreases the collision rate due to their repulsive nature. On further adding the momentum and symmetry potential, collision rate decreases upto some extent and then remains constant.

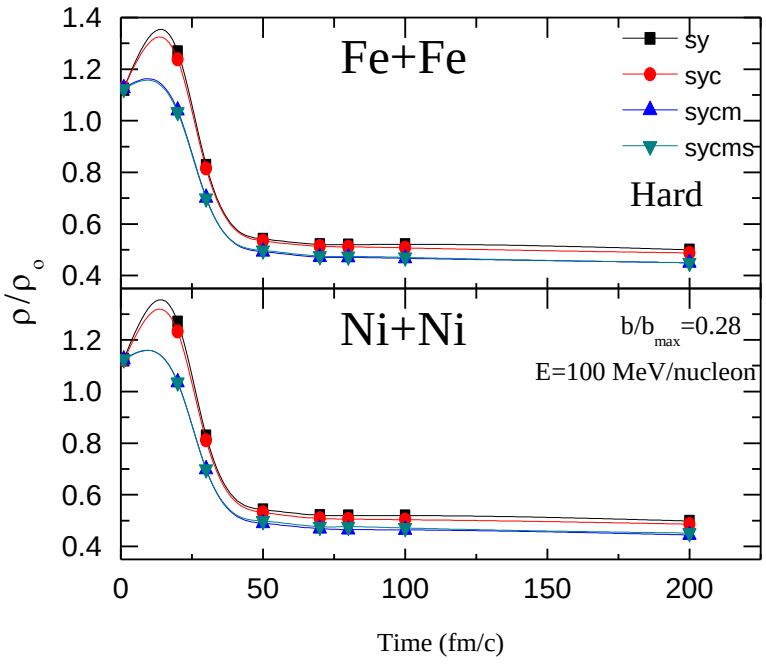

FIG.3.1. Time evolution of density for reduced impact parameter ($b/b_{max} = 0.28$) at 100 MeV/nucleon for the systems $^{58}_{28}$Ni + $^{58}_{28}$Ni and $^{58}_{26}$Fe + $^{58}_{26}$Fe .

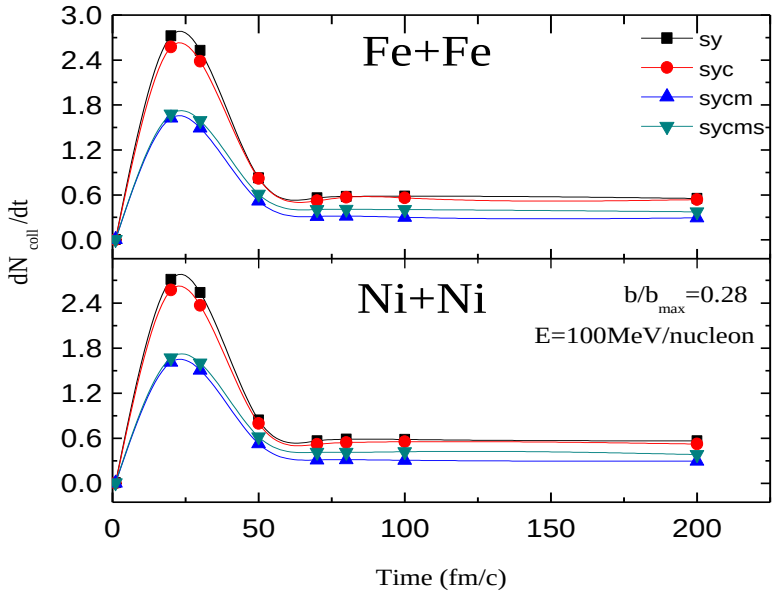

FIG.3.2. Allowed collisions as a function of time for impact parameter ($b/b_{max} = 0.28$) at 100 MeV/nucleon.

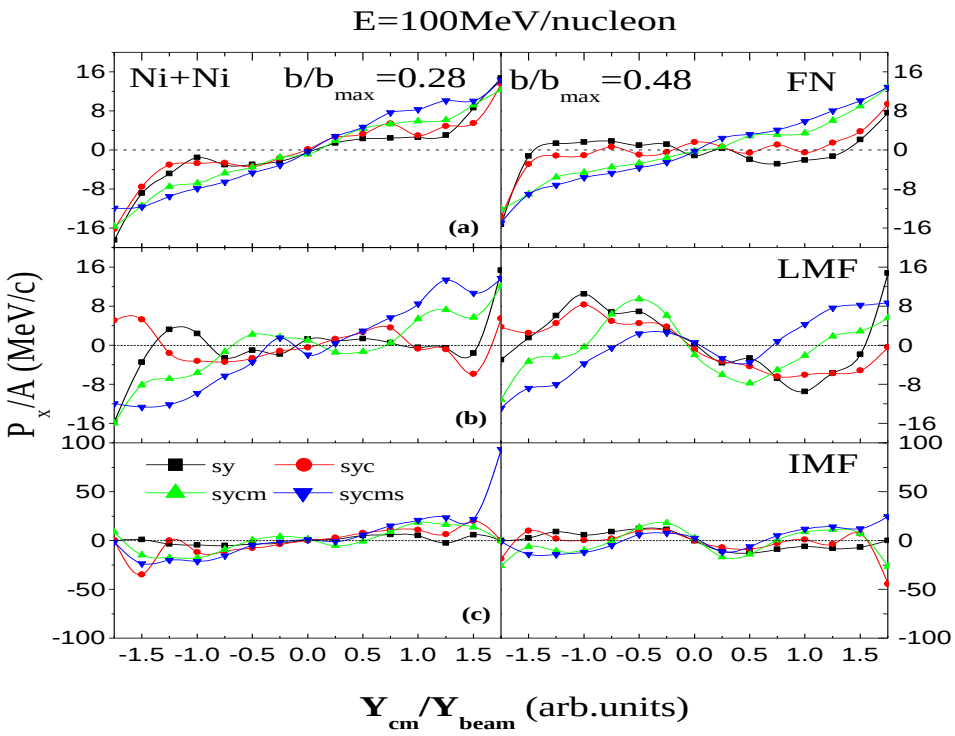

FIG.3.3. Average transverse momentum in reaction plane versus reduced center of mass rapidity from semicentral collisions ($b/b_{max} = 0.28, 0.48$) at 100 MeV/nucleon for $^{58}_{28}$Ni + $^{58}_{28}$Ni for a) FN b) LMF c) IMF.

Fig.3.3, shows the average transverse momentum in reaction plane $< P_X/A >$ plotted versus the reduced c.m.rapidity (Y_{cm}/Y_{beam}) for $^{58}_{28}$Ni + $^{58}_{28}$Ni at two impact parameters at 100 MeV/nucleon for different potentials. The results are shown for free nucleon (FN), light mass fragment (LMF) and intermediate mass fragment (IMF). The data exhibit the characteristic " S-shape" associated with collective transverse flow in the reaction plane. As the impact parameter increases, transverse flow increases, passes through a maxima and diminishes for most peripheral impact parameters. Different colors and symbols are indicating different potentials.

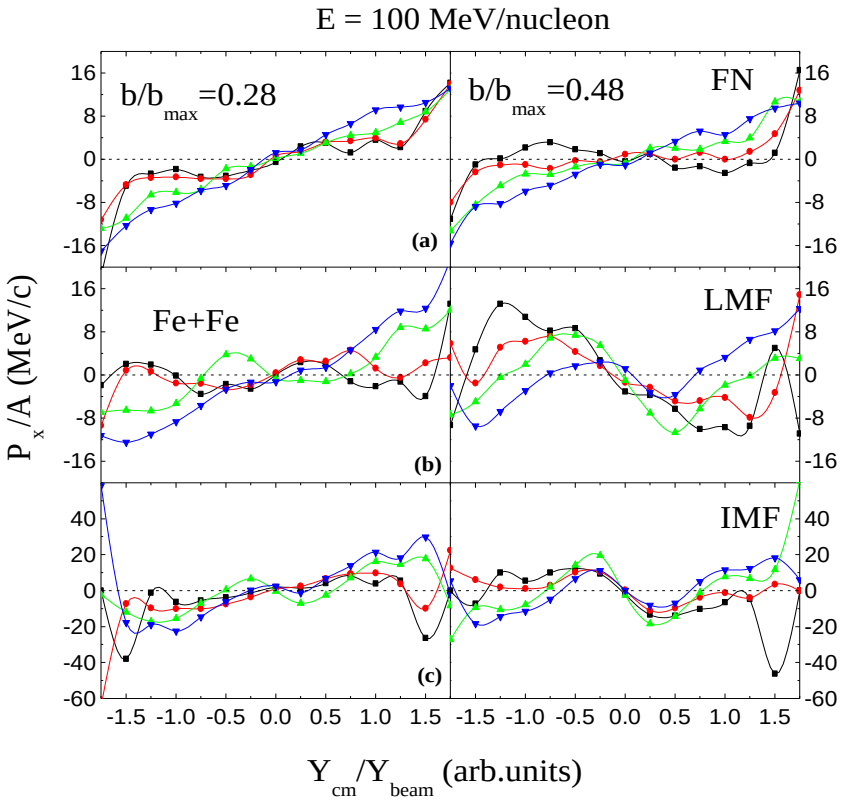

FIG.3.4. Average transverse momentum in reaction plane versus reduced center of mass rapidity from semicentral collisions ($b/b_{max} = 0.28, 0.48$) at 100 MeV/nucleon for $^{58}_{26}$Fe + $^{58}_{26}$Fe for a) FN b) LMF c) IMF.

Figure.3.4. shows the average transverse momentum in reaction plane $< P_X/A >$ plotted versus the reduced c.m.rapidity (Y_{cm}/Y_{beam}) for $^{58}_{26}$Fe + $^{58}_{26}$Fe for two impact parameters at 100 MeV/nucleon for different potentials. The calculations exhibit the characteristic " S-shape" associated with collective transverse flow in the reaction plane. As the impact parameter increases, transverse flow increases, passes through a maxima and diminishes for most peripheral impact parameter.

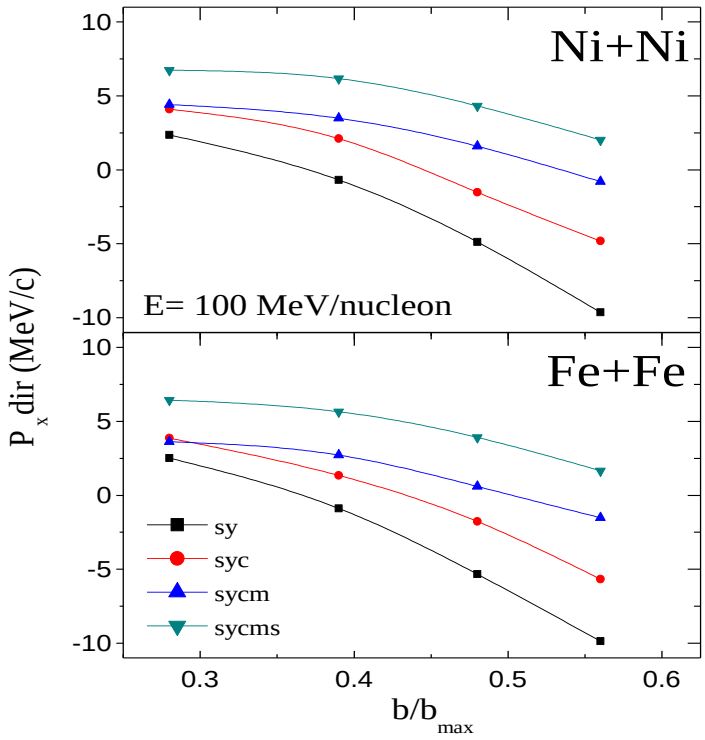

FIG.3.5. Directed transverse flow as a function of the reduced impact parameter from $^{58}_{26}$Fe + $^{58}_{26}$Fe and $^{58}_{28}$Ni + $^{58}_{28}$Ni at 100 MeV/nucleon.

Figure.3.5, shows the directed transverse flow as a function of reduced impact parameter for the systems $^{58}_{26}$Fe + $^{58}_{26}$Fe and $^{58}_{28}$Ni + $^{58}_{28}$Ni at 100 MeV/nucleon. The neutron-rich system $^{58}_{26}$Fe + $^{58}_{26}$Fe systematically exhibits larger flow values than $^{58}_{28}$Ni + $^{58}_{28}$Ni at all the reduced impact parameters displayed. On adding the potentials step by step to sy (Skyrme + Yukawa) flow increases with impact parameter. The largest difference in the magnitude of the flow between the entrance channels occurs for heavier mass fragments at semicentral collisions.

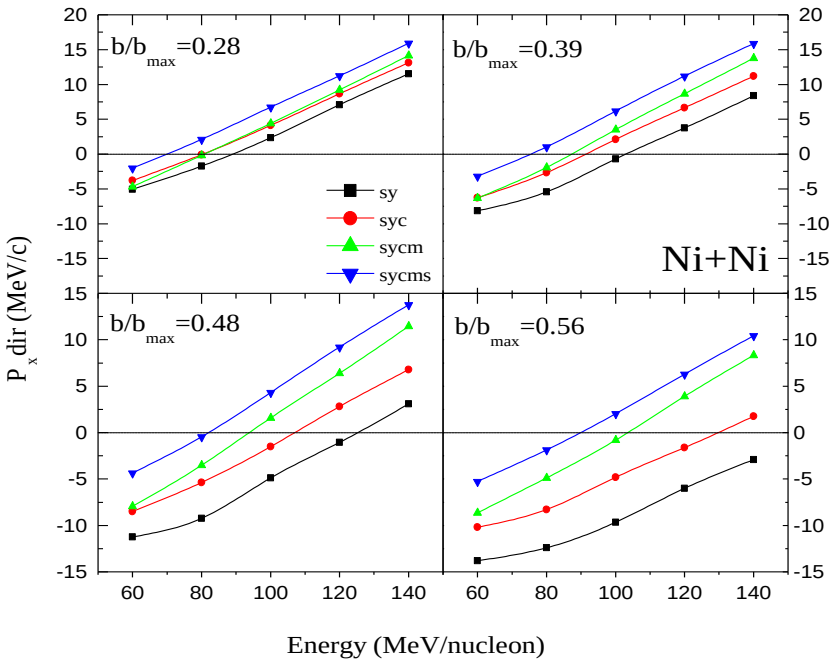

FIG.3.6. Directed transverse flow as a function of energy from $^{58}_{28}$Ni + $^{58}_{28}$Ni at different impact parameters.

Figure.3.6. shows the directed transverse flow as a function of energy for $^{58}_{28}$Ni + $^{58}_{28}$Ni at different impact parameters as shown in the figure above. It is clear from the figure that the value of directed flow decreases with increase in the energy. Different symbols and colors represents different kinds of potentials. On adding Coulomb potential to Skyrme +Yukawa potential the flow value decreases. Further on adding momentum and symmetry potential to syc (Skyrme + Yukawa + Coulomb), the flow value is smaller as compared to sy.

Figure.3.7. shows the directed transverse flow as a function of energy for $^{58}_{26}$Fe + $^{58}_{26}$Fe at different impact parameters. It is seen that the result for $^{58}_{26}$Fe + $^{58}_{26}$Fe is coming almost equivalent to $^{58}_{28}$Ni + $^{58}_{28}$Ni.

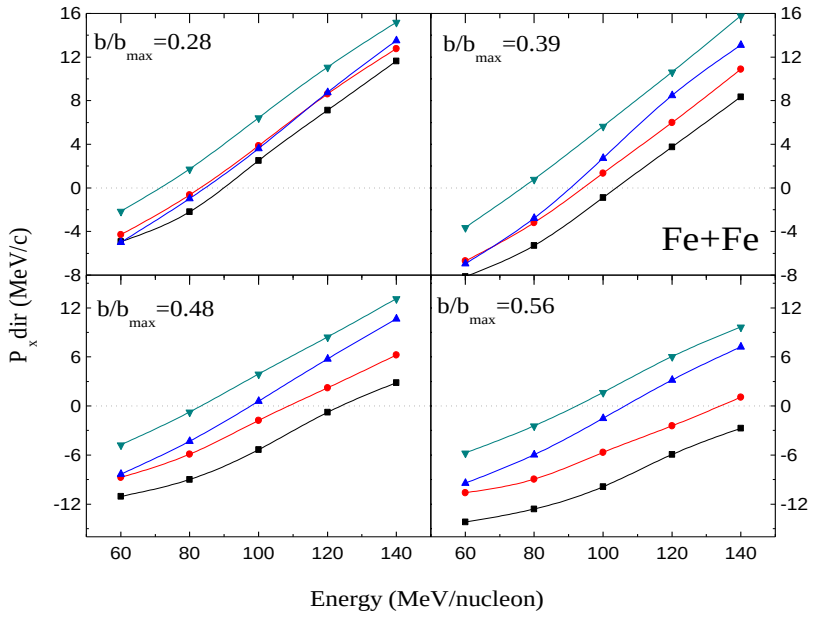

FIG.3.7. Directed transverse flow as a function of energy from $^{58}_{26}$Fe + $^{58}_{26}$Fe at different impact parameters.

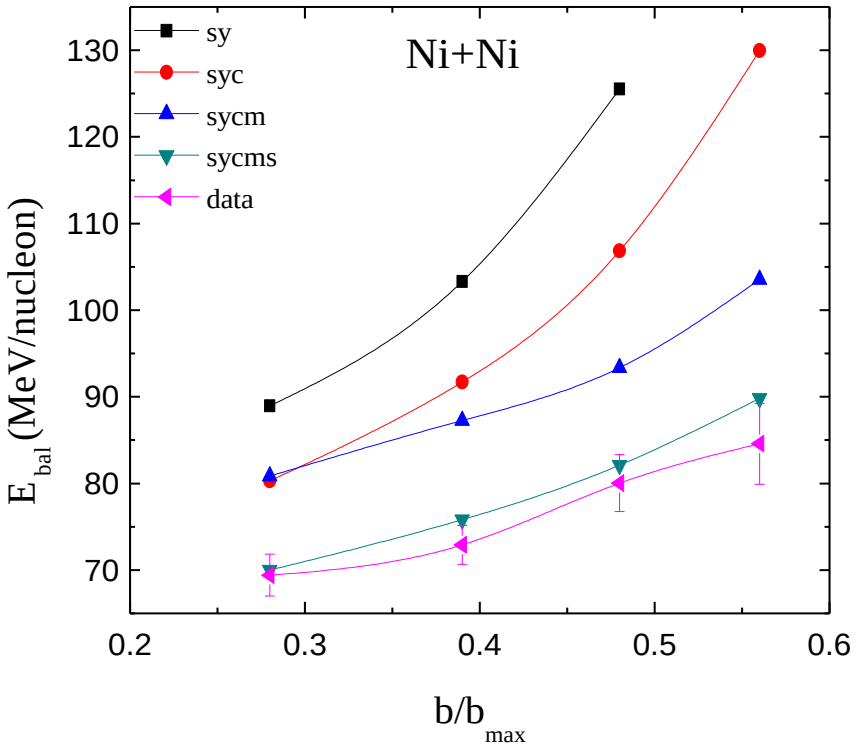

FIG.3.8. E_{bal} as a function of impact parameter for the system $^{58}_{28}$Ni + $^{58}_{28}$Ni.

In figure.3.8. we display the E_{bal} as a function of impact parameter for the system $^{58}_{28}$Ni + $^{58}_{28}$Ni. We also display the experimental data [13] and our corresponding calculations in the range of colliding geometry used in present study. Also we are using hard equation of state. It is clear from the figure that E_{bal} increases with increase in impact parameter.

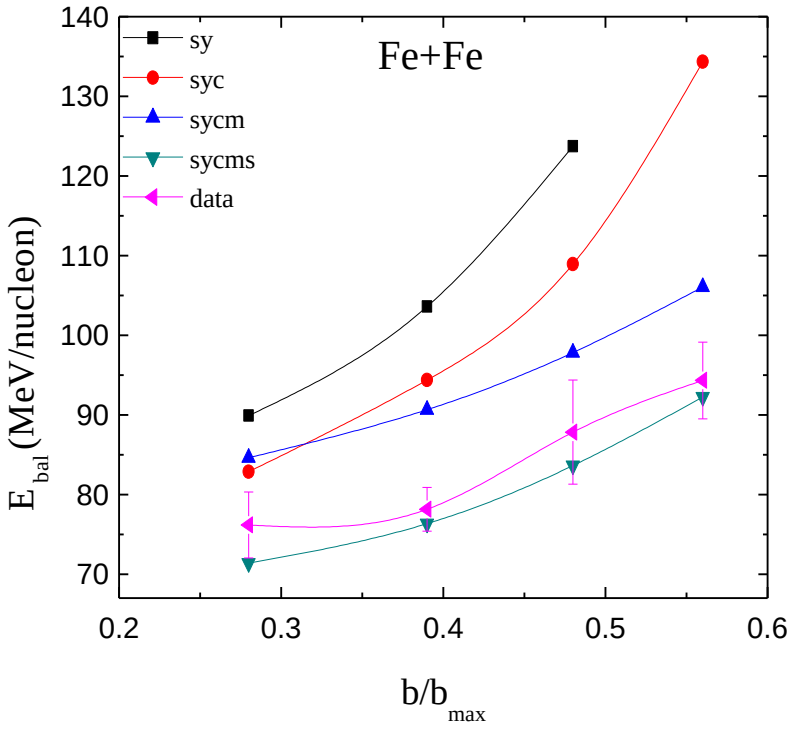

FIG.3.9. E_{bal} as a function of impact parameter for the system $^{58}_{26}$Fe + $^{58}_{26}$Fe.

Figure.3.9. shows E_{bal} as a function of impact parameter for the system $^{58}_{26}$Fe + $^{58}_{26}$Fe. Here we are taking the values of E_{bal} for different kinds of potentials shown in the figure above. It is seen that the increase in E_{bal} is more in $^{58}_{26}$Fe + $^{58}_{26}$Fe than $^{58}_{28}$Ni + $^{58}_{28}$Ni. Clearly our results are in good agreement with the data.

Figure.3.10. shows ΔE_{bal} as a function of impact parameter for the system $^{58}_{28}$Ni + $^{58}_{28}$Ni. It is clear from the figure that the contribution of symmetry potential is very less so we are getting a linear line drawn as blue line in figure.

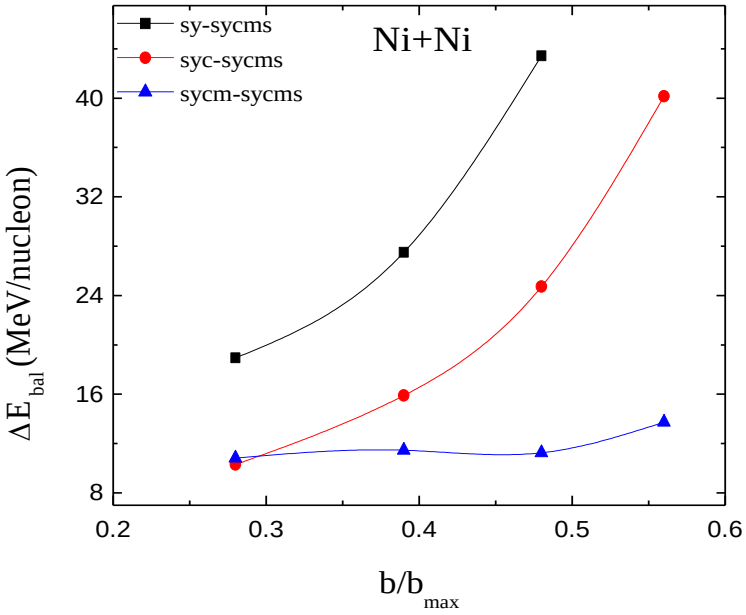

FIG.3.10. ΔE_{bal} as a function of impact parameter for the system $^{58}_{28}$Ni + $^{58}_{28}$Ni.

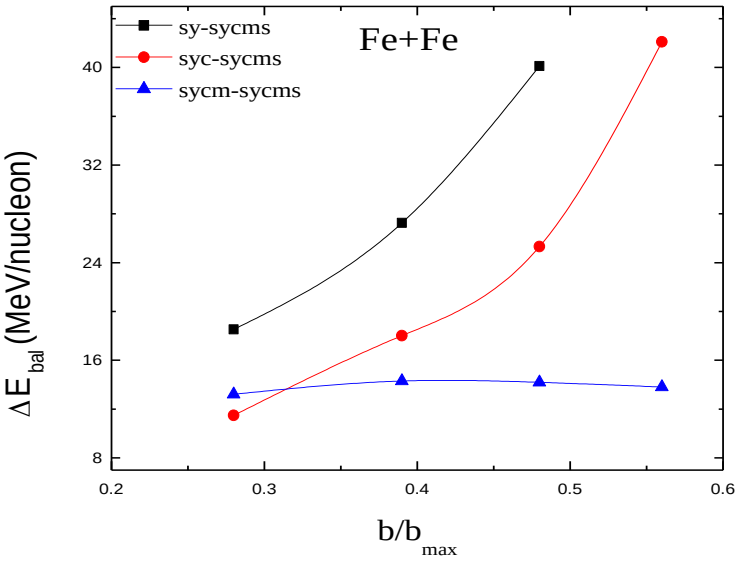

FIG.3.11. ΔE_{bal} as a function of impact parameter for the system $^{58}_{26}$Fe + $^{58}_{26}$Fe.

Figure.3.11, shows ΔE_{bal} as a function of impact parameter for the system $^{58}_{26}$Fe + $^{58}_{26}$Fe. ΔE_{bal} increases with increase in impact parameter with and without Coulomb potential but there is small variation for difference in sycm and sycms.

3.3 Summary

The thesis contains a brief review of one of the important branch of nuclear physics i.e. heavy ion physics. It also contains the theoretical study of directed flow. The isospin dependent quantum molecular dynamics model (IQMD) is used to describe the directed flow for asymmetric colliding nuclei for heavy ion reactions.

In chapter 2 isospin dependent quantum molecular dynamics model is explained in detail. Then method of clusterization i.e. minimum spanning tree method is also discussed.

In chapter 3 there is complete study of directed flow and balance energy for different potentials in heavy ion collision in the energy range between 60 MeV/nucleon and 140 MeV/nucleon by using hard equation of state. Rapidity distribution, dependence of energy and impact parameter are shown in figures for different potentials.

3.4 References:

[1] L. C. Vaz, J. M Alexander & G. R Satchler, Phys. Rep. **69**, 373 (1981); M Beckerman, Rep. Prog. Phys. **51**, 1047 (1988).

[2] K. E. Zyromski *et al.*, Phys. Rev. C **55**, R562 (1997).

[3] Sakshi Gautum, Aman D. Sood, Rajeev K. Puri and J. Aichelin, Phys. Rev. C **83**, 014603 (2011).

[4] J. Aichelin *et al*., private communication.

[5] S. Hundan *et al*, Phys. Rev. C **71**, 054604 (2005).

[6] Ch. Hartnack, Rajeev K. Puri, J. Aichelin, J. Konopka, S. A. Bass, H. Stocker, W. Greiner, Eur. Phys. J. A **1**, 151 (1998).

[7] D. Benchekroun *et al*., Z. Phys. A **356**, 411 (1997).

[8] P. Danielewicz and G. F. Bertsch, Nucl. Phys. A **533**, 712 (1991).

[9] S. Huber and J. Aichelin, Nucl. Phys. A **573**, 587 (1994).

[10] J. Singh, S. Kumar and R. K. Puri, Phys. Rev. C **62**, 044617 (2000); *ibid* 65, 024602 (2002); R.K Puri and S. Kumar, Phys. Rev. C **57**, 2744 (1998).

[11] S. Kumar, S. Kumar and R.K. Puri, Phys. Rev. C **81**, 014611 (2010).

[12] S. Voloshin, Phys. Rev. C **55**, R1630 (1997).

[13] R. Pak *et al.*, Phys. Rev. Lett. **78**, 6 (1997).